Bulletin of the Earthquake
Research Institute
Vol. 41 (1963), pp. 761-779

46. *Study on the Crust-mantle Structure in Japan.**

Part 2, Interpretation of the Results Obtained by Seismic Refraction Studies in Connection with the Study of Gravity and Laboratory Experiments.

By Hiroo KANAMORI,

Geophysical Institute, Faculty of Science,
The University of Tokyo.

(Read June 25, 1963.—Received Sept. 26, 1963.)

Abstract

The crustal and upper mantle structures determined by the Research Group for Explosion Seismology (R.G.E.S.) have been interpreted in view of gravity indications and laboratory experiments.

The structures determined by the time-distance curves in the refraction studies were based on the assumption that there is no masked layer within the crust. They do not seem to conform well to either the results of the gravity analysis or surface wave studies. If the second layer, which has not been revealed by the refraction studies, is taken into account, the situation becomes much better. This fact leads us to suspect that, 1) there may be a layer of larger compressional wave velocity (6.6~6.7 km/sec) in the lower part of the crust, or there may be a velocity increase towards the base of the crust. 2) The mean crustal density and the vertical velocity distribution may not be very different from those of the standard continental crust. 3) An intermediate layer may exist just below the Moho discontinuity though the physical and geometrical structure of the layer remains uncertain. Adopting the crustal sections described above, the most probable depth of the Mohorovičić discontinuity in every 1° square on land defined in Part 1 of this study has been determined from the reduced Bouguer anomalies.

1. Results by explosion studies

The Research Group for Explosion Seismology (R.G.E.S.) has carried out several successful observations of seismic waves generated by

* Communicated by T. HAGIWARA.

artificial explosion in various districts in Japan.

Several crustal and upper mantle models derived from their studies have been presented. Although there are several minor differences between a structure in one district and that in another, there are characteristic features common to them all. They are as follows. 1) Low compressional wave velocity α in the crust; the vertical velocity profile in the crust is such that there is a thin upper layer in which α is about 5.5 to 5.8 km/sec underlain by a lower layer in which α is about 6.0 km/sec. The ratio of the thickness of the upper layer to that of the lower layer is about 1 : 8 to 2 : 8 on the average. 2) Low mantle velocity compared with the continental mantle velocity. Compressional wave velocity α for the upper mantle, which has been obtained, varies widely from place to place, and the range of the variation seems to be from 7.5 km/sec to 7.9 km/sec, which is substantially lower than the normal mantle velocity in the continent. 3) The average thickness of the crust is about 25 km in Tohoku district, about 30 km in Kanto district, about 36 km in Chubu district and about 28 km in Chugoku district.

It should be noted here that the structures derived from the time-distance curves are much affected by the assumption on the geometrical configuration of the structure which is made prior to the analysis. As a consequence, the complex structure under Japanese Islands makes the deduction of the detailed structure from the observed time-distance curve very difficult. This may particularly be the case in Chubu and Tohoku districts where the crustal structure is suspected, from the gravity analysis, to vary sharply from place to place. From this consideration, the average structures given by R.G.E.S. (Model 2) have been adopted in this study with slight modifications.

In order to interpret the seismic structures in view of gravity data, it appears more desirable to select the profiles along which the gravity value does not change abruptly. Hence, the profiles in Chubu and Tohoku districts were not taken into account in the present study.

According to the reduced Bouguer anomaly ΔG obtained in Part 1 of this study,[1] the structure in the western portion of the area studied by Miboro explosion (1957) (Fig. 1) is much simpler than those along other profiles. The above indication suggests that the western profiles A and B of Miboro explosion should be adopted as the typical crustal model in Japan for the present purpose. Application of the procedures

1) H. KANAMORI, *Bull. Earthq. Res. Inst.*, **41** (1963), 743-759.

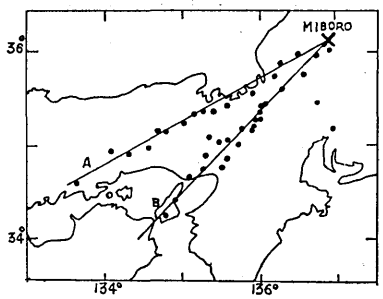

Fig. 1. Western profiles A, B of the Miboro Explosion (1957). (after R.G.E.S.)

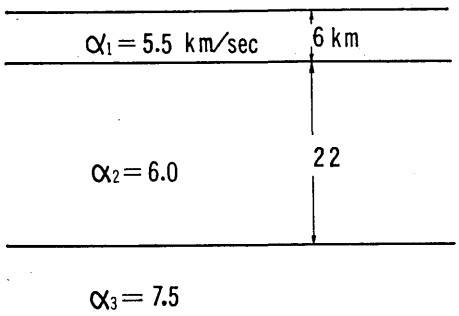

Fig. 2. Modified crustal structure deduced from the first arrival of seismic waves from the Miboro Explosion (1957). α_i denotes compressional wave velocity in the i-th layer.

followed in the present study to other parts of Japan would be almost prohibitive owing to the complicated nature of the structures. Therefore the results from Chugoku district will be extended to other districts: the consistency of the results with those obtained by other methods will justify this extension.

The characteristic features of the structure in this district, obtained by R.G.E.S., are given by Fig. 2.[2),3),4)] (Modified from their Model 2 in western profile).

2. Laboratory data

In order to combine the seismic data with those of gravity, it is important to know the relationship between density ρ and compressional wave velocity α of various rocks forming structures. Several attempts have been made to obtain a reasonable relationship between ρ and α for various values of ρ.[5),6)] However, since the fluctuation of the values determined for an individual rock sample is comparatively large, the direct application of the fixed curves connecting ρ with α to a problem of this kind appears to be misleading. In this question we have based

2) T. MIKUMO, M. OTSUKA, T. OTSU, T. TERASHIMA and A. OKADA, *Bull. Earthq. Res. Inst.*, **36** (1961), 327-349.

3) THE RESEARCH GROUP FOR EXPLOSION SEISMOLOGY, *Zisin*, **14** (1961), 150, (in Japanese).

4) THE RESEARCH GROUP FOR EXPLOSION SEISMOLOGY, *Zisin*, **14** (1968), 168, (in Japanese).

5) G. P. WOOLLARD, *J. Geophys. Res.*, **64** (1959), 1521.

6) J. E. NAFE and C. L. DRAKE, unpublished. See e.g., M. TALWANI, J. L. WORZEL and M. EWING, *J. Geophys. Res.*, **66** (1961), 1265.

Table 1. Number of various rock samples classified by density ρ (g/cm^3) and compressional wave velocity α (km/sec) under the confining pressure of 6000 bars. (from the Table given by Birch)

(P=6000 bars) α km/sec	ρgm/cc 2.55 ~2.65	2.65 ~2.75	2.75 ~2.85	2.85 ~2.95	2.95 ~3.05	3.05 ~3.15	3.15 ~3.25	3.25 ~3.35	3.35 ~
5.50~5.70	0	2	0	0	0	0	0	0	0
5.70~5.90	2	2	0	0	0	0	0	0	0
5.90~6.10	2	6	1	0	0	0	0	0	0
6.10~6.30	11	8	2	0	0	0	0	0	0
6.30~6.50	13	18	2	0	1	0	0	0	0
6.50~6.70	0	9	10	3	3	0	0	0	0
6.70~6.90	0	2	8	2	13	1	0	0	0
6.90~7.10	0	0	6	1	1	0	1	0	1
7.10~7.30	1	0	4	1	4	2	0	0	1
7.30~7.50	0	0	1	1	0	0	0	1	1
7.50~7.70	0	0	0	0	0	2	2	2	3
7.70~7.90	0	0	0	0	0	0	3	8	4
7.90~8.10	0	0	0	0	0	0	2	4	6
8.10~8.30	0	0	0	0	0	0	3	2	0
8.30~	0	0	0	0	0	0	0	7	2

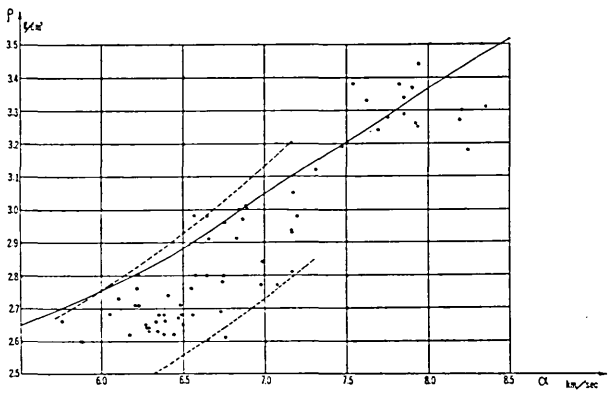

Fig. 3. Compressional wave velocity α at 6000 bars versus density ρ for various rock specimens. The points are plotted from the Table given by Birch (1960). Solid line shows the relation between ρ and α given by Nafe and Drake, and dashed lines show the possible range of the variation in ρ for various values of α.

our study on the data given by Birch.[7] In Table 1, rocks of various kinds are classified by density ρ and compressional wave velocity α under the confining pressure of 6000 atmospheric pressures. The integer in this table stands for the number of abundance in Birch's table. Also in Fig. 3, the values for individual measurement are plotted with α as abscissa and ρ as ordinate. For comparison, we have included here the curve representing the ρ-α relation given by Nafe and Drake. It can be seen from this figure that, while the curve approximates the data fairly well, the individual measurement fluctuates about the curve appreciably and the curve does not seem to fit the data well at the lower velocity and density part. What we can safely conclude from Fig. 3 and Table 1 is that the ρ-α relation holds only approximately and allowance should always be made for a range in ρ for given α, i.e.,

$$\begin{array}{lllll} & \text{if} & \alpha=6.0\ \text{km/sec} & \text{then} & 2.40<\rho<2.75\ \text{g/cm}^3, \\ & \text{if} & \alpha=6.3\ \text{km/sec} & \text{then} & 2.50<\rho<2.85\ \text{g/cm}^3, \\ & \text{if} & \alpha=6.6\ \text{km/sec} & \text{then} & 2.60<\rho<3.00\ \text{g/cm}^3, \\ & \text{if} & \alpha=6.9\ \text{km/sec} & \text{then} & 2.70<\rho<3.10\ \text{g/cm}^3, \\ \text{and} & \text{if} & \alpha=7.2\ \text{km/sec} & \text{then} & 2.80<\rho<3.20\ \text{g/cm}^3, \end{array} \qquad (1)$$

3. Interpretation

3.1. Gravity data

In general, Bouguer anomalies represent mass anomalies in the crustal and mantle layering ; a positive Bouguer anomaly indicates that the crustal column has an excess of mass regardless of its layering. If we adopt the standard crustal section given by Worzel and Shurbet,[8] it follows from the above consideration that if the Bouguer anomaly is zero in a crustal column A of height H_A and of mean density ρ, H_A and ρ should be related by,

$$\rho_M(H_S-H_A)+\rho H_A=\rho_O H_S, \qquad (2)$$

where H_S and ρ_O denote the height and mean density of the standard crust given by Worzel and Shurbet and ρ_M is the mean density of the mantle taken as constant. From Formula (2), if the mean crustal density is decreased by $\Delta\rho$ from that of the standard crust, the thickness of the crust should be decreased by,

7) F. BIRCH, *J. Geophys. Res.*, **65** (1960), 1083.

8) J. L. WORZEL and G. I. SHURBET, *Crust of the Earth* (Geol. Soc. Am. 1955).

$$\Delta H_A = H_S - H_A = \frac{\rho - \rho_C}{\rho - \rho_M} H_S = \frac{\Delta\rho}{(\rho_M - \rho_C) + \Delta\rho} H_S \ . \qquad (3)$$

The foregoing discussion can be generalized to a crustal column A' which has an intermediate layer just below the Moho. Let H_I be the thickness of the intermediate layer of density ρ_I, then $H_{A'}$ can be given by the following,

$$H_{A'} = \frac{\rho_M - \rho_C}{\rho_M - \rho} H_S + \frac{\rho_I - \rho_M}{\rho_M - \rho} H_I \ ,$$

and

$$\Delta H_{A'} = H_S - H_{A'} = \frac{\Delta\rho}{(\rho_M - \rho_C) + \Delta\rho} H_S + \frac{\rho_M - \rho_I}{(\rho_M - \rho_C) + \Delta\rho} H_I \ ,$$

$$= \Delta H_A + \frac{\rho_M - \rho_I}{(\rho_M - \rho_C) + \Delta\rho} H_I \ . \qquad (4)$$

From Equations (3) and (4), it can be said that the density decrease in the crust brings Moho up to compensate the resulting mass deficiency in the crust by the heavier mantle material, and the existence of the intermediate layer in which the density ρ_I is smaller than the normal mantle density ρ_M will result in further uplift of the Moho.

The Bouguer anomalies along the western profiles of Miboro explosion are approximately zero as shown in Fig. 1 of Part 1 of this study.[9] We can, therefore, apply the foregoing discussion and Formulas (3) and (4) to the crustal column in this area.

If the intermediate layer is not taken into account, the crustal thickness H can be deduced from Formula (2) with the value for $\rho_C = 2.84\ \mathrm{g/cm^3}$, $\rho_M = 3.27\ \mathrm{g/cm^3}$, $H_S = 33$ km given by Worzel and Shurbet and ρ which should be estimated by other methods. If we adopt the structure determined by R.G.E.S. (Fig. 2 a, b) the mean compressional wave velocity α in the crust is about 6 km/sec, which suggests that the mean density of the crustal material should be less than $2.75\ \mathrm{g/cm^3}$, as discussed in Section 2. With this value, the crustal thickness H is evaluated as,

$$H < \frac{0.43}{3.27 - 2.75} 33 = 27.3\ \mathrm{km}.$$

9) H. KANAMORI, *loc. cit.*, 1).

Although this value does not contradict the one deduced from the refraction studies (28 km), it is felt that the result might not be convincing enough for the following reasons.

The result obtained above from the gravity indications may give the upper limit of H, and the possible existence of the intermediate layer, which has been strongly suggested by the low mantle velocity in the upper mantle, would make it smaller by 1 to 2 km as mentioned earlier, and the most probable thickness would be reduced to about 25 km or less. On the contrary, the thickness of the crust deduced by the seismic refraction method generally gives the lower limit of the crust, as will be shown in Section 3.3., due to the masking effect of crustal layering.

A more comprehensive structure which agrees with the results by both the gravity and seismic methods, if any such exists, should be investigated.

3.2. Phase velocity data

Phase velocity of Rayleigh wave in this region has been determined by Kaminuma and Aki.[10),11)] It is of interest to compare the results given by R.G.E.S. to those obtained by the surface wave study.

For the computation of theoretical phase velocity dispersion curves, we have adopted the crustal models J-II-1 and J-II-1′ which are based on the structure given by R.G.E.S. and shown by Fig. 4 a,b. In J-II-1 model, Poisson's ratio is taken as $\sigma=0.25$ and for J-II-1′, $\sigma=0.27$ is adopted. The dispersion curves have been computed by the method developed by Takeuchi, Saito and Kobayashi[12)] for NEAC 2203 computer. The solid lines in Fig. 5 show the phase velocity C versus $1/kH$, where k is the wave number and H is the total thickness of the crust. The phase velocities of Rayleigh waves in this area given by Kaminuma

J-II-1

α	β	ρ	σ	H
5.5	3.18	2.67	0.25	1
6.0	3.46	2.90	0.25	3
7.5	4.33	3.27	0.25	∞

a

J-II-1′

α	β	ρ	σ
5.5	3.08	2.67	0.27
6.0	3.36	2.90	0.27
7.5	4.21	3.27	0.27

b

Fig. 4. Layer parameters for crustal model J-II-1 (a) and J-II-1′ (b). (α; compressional wave velocity in km/sec, β; shear velocity in km/sec, ρ: density in g/cm^3, σ; Poisson's ratio, H; dimensionless thickness)

10) K. Aki, *Bull. Earthq. Res. Inst.*, **39** (1961), 255.
11) K. Kaminuma and K. Aki, *ibid.*, **41** (1963), 243.
12) H. Takeuchi, M. Saito and N. Kobayashi, *Zisin*, **14** (1961), 217, (in Japanese).

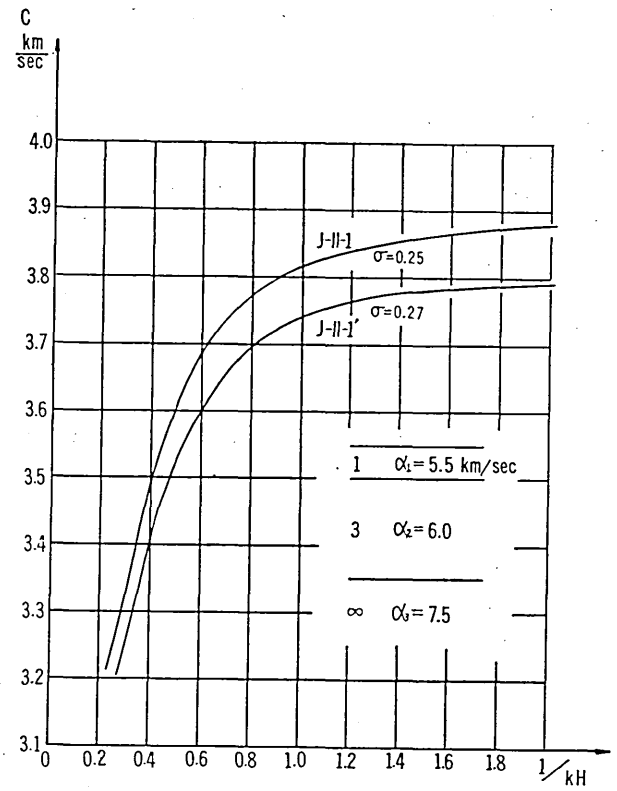

Fig. 5. Rayleigh wave phase velocity dispersion curves for crustal models J-II-1 and J-II-1′. Solid lines indicate the relation between phase velocity C and kH, where k is the wave number and H is the total thickness of the crust. (i.e. $H=H_1+H_2$)

Table 2. The value of phase velocity of Rayleigh waves in Chugoku district. (Reproduced from Kaminuma and Aki)

Wave No.	Period	Phase velocity C
1	41.3 sec.	3.784±0.106 km/sec.
2	32.1	3.715±0.056
3	27.4	3.764±0.087
5	24.8	3.649±0.102
7	23.0	3.608±0.154

and Aki are tabulated with probable errors in Table 2. With this data, determination of the crustal thickness can be made using the dispersion curves given in Fig. 5 by the least square method as made by Kaminuma

and Aki. The results are $H=25$ km and $H=17$ km corresponding to the case of $\sigma=0.25$ and $\sigma=0.27$ respectively.

Although there is no compelling reason for adopting 0.25 or 0.27 for σ, the laboratory measurements for some rocks have shown[13] that,

$$\text{for granite} \quad \sigma=\begin{cases}0.258\\0.253\\0.269\end{cases},$$

$$\text{for gabbro} \quad \sigma=\begin{cases}0.314\\0.273\end{cases},$$

$$\text{for dunite} \quad \sigma=0.269\ .$$

This implies that the Poisson's ratio for granite is about 0.26, at least larger than 0.25, and the basic rocks generally have a larger Poisson's ratio which appears to be about 0.27 or even larger. Therefore, $H=25$ km deduced with $\sigma=0.25$ may give the upper limit, and $H=17$ km, with $\sigma=0.27$ the average value, which are both too small to conform to the results by the explosion study. This fact again suggests either that the possible masked layers within the crust which have not been revealed by the refraction study exist, or that the velocity in the layer just below the Moho discontinuity gradually increases to the normal mantle velocity downward, or both.

As is clear from this example, the phase velocity data limited in period range will often give very different results depending on the slight difference in the assumed structures.

3.3. Masking of layering

The foregoing section suggests the existence of another layer within the crust. In this section an attempt is made to reveal the masked layer and to obtain a crustal structure which would be consistent with the evidence from gravity, explosion and surface wave studies.

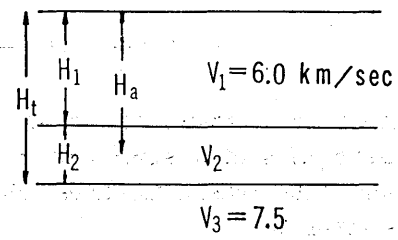

Fig. 6. Schematic representation for a two-layered crustal structure in which the second layer is masked in the analysis of the first arrival of refracted waves.

In the following analysis, the author intends to eliminate one possible

13) F. BIRCH, *J. Geophys. Res.*, **66** (1961), 2199.

structure after another finally leaving a few indispensable structures which cannot be excluded.

If we take a crustal layering given by Fig. 6, the second layer would not yield the first arrival in the time-distance curve of refracted waves, unless the following condition is met.

$$\frac{H_1}{H_2}\frac{v_2}{v_1}\left[\frac{(v_3-v_1)}{(v_2-v_1)}\cdot\frac{(v_2^2-v_1^2)^{1/2}}{(v_3^2-v_1^2)^{1/2}}-1\right]<\left(\frac{v_3^2-v_2^2}{v_3^2-v_1^2}\right)^{1/2}, \tag{5}$$

where v_1, v_2 and v_3 denote the wave velocity in the first, second and third layer respectively, and H_1, H_2 represent the thickness of the corresponding layer. In the present case, if we assume the existence of the masked second layer and assign the values for $v_1=6.0$km/sec, $v_3=7.5$km/sec, the time-distance curve of the direct and refracted waves would be as shown by Fig. 7. The segments, I, II and III in Fig. 7 which represent the direct and refracted waves from the second and third layer respectively can be given by,

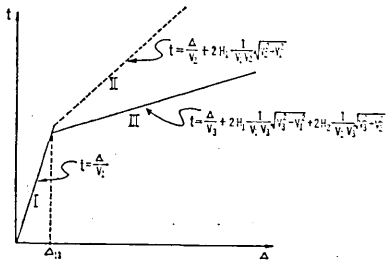

Fig. 7. Typical time-distance curve for the structure described in Fig. 6.

$$\text{I}\qquad t=\frac{\Delta}{v_1}, \tag{6}$$

$$\text{II}\qquad t=\frac{\Delta}{v_2}+2H_1\left(\frac{\sqrt{v_2^2-v_1^2}}{v_1 v_2}\right), \tag{7}$$

$$\text{III}\qquad t=\frac{\Delta}{v_3}+2H_1\frac{1}{v_1 v_3}\sqrt{v_3^2-v_1^2}+2H_2\frac{1}{v_2 v_3}\sqrt{v_3^2-v_2^2}. \tag{8}$$

Since the crustal thickness deduced by R.G.E.S. is based on the assumption of a single layer crust (the superficial layer is neglected here), the crustal thickness obtained is the apparent thickness H_a which is given by,

$$H_a=\frac{1}{2}\Delta_{13}\left(\frac{v_3-v_1}{v_3+v_1}\right)^{1/2}, \tag{9}$$

where Δ_{13} is the distance of the intersection of segment I and III. From (6) and (7), eliminating t, we obtain,

$$H_1=\frac{1}{2}\Delta_{13}\left(\frac{v_3-v_1}{v_3+v_1}\right)^{1/2}-\frac{v_1}{v_2}\left(\frac{v_3^2-v_2^2}{v_3^2-v_1^2}\right)^{1/2}H_2=H_a-\frac{v_1}{v_2}\left(\frac{v_3^2-v_2^2}{v_3^2-v_1^2}\right)^{1/2}H_2\,. \tag{10}$$

Whereupon the true thickness of the crust H_t can be given, with H_2 as a parameter, by,

$$H_t=H_1+H_2=H_a+H_2\left\{1-\frac{v_1}{v_2}\left(\frac{v_3^2-v_2^2}{v_3^2-v_1^2}\right)^{1/2}\right\}. \tag{11}$$

The critical value of H_t, beyond which the second layer would not be masked, can be obtained by combining (5), (9), (10) and (11), as,

$$H_{tc}=\left(\frac{v_3+v_1}{v_3-v_1}\right)^{1/2}\left(\frac{v_2-v_1}{v_2+v_1}\right)^{1/2}(1+\kappa_c), \tag{12}$$

where

$$\kappa_c=\frac{v_2}{v_1}\left[\frac{(v_3-v_1)}{(v_2-v_1)}\frac{(v_2^2-v_1^2)^{1/2}}{(v_3^2-v_1^2)^{1/2}}-1\right]\left(\frac{v_3^2-v_1^2}{v_3^2-v_2^2}\right)^{1/2}.$$

In Fig. 8, H_t and H_{t_c} are plotted for various values of v_2 ranging from 6 km/sec ($=v_1$) to 7.5 km/sec ($=v_3$) and H_2 from 0 to 15 km with the fixed value of $H_a=28$ km which has been determined by R.G.E.S.. From this figure, it can readily be seen that with a fixed value of v_2, the true thickness H_t will increase as the thickness H_2, and with a fixed value of H_2, H_t increases with v_2. However, H_t cannot exceed 33 km (in the case where $H_a=28$ km) so long as the second layer is assumed to be masked.

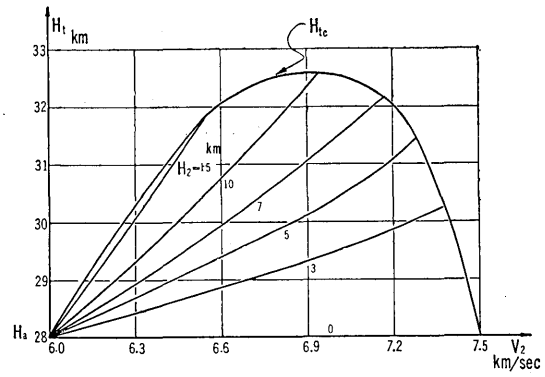

Fig. 8. True thickness $H_t=H_1+H_2$ for various values of velocity in the second layer v_2, with the thickness of the second layer H_2 as a parameter. The apparent thickness H_a is fixed at the value determined by R.G.E.S.. The upper limit of H_t is determined by H_{t_c} given in the figure by a convex curve.

Now we have determined the possible range of the variations in the values of v_2 and H_2 which does not violate the observed time-distance curve of the first arrival of seismic waves given by R.G.E.S.. In order

to determine these values more accurately the gravity data should be taken into account.

The Bouguer anomaly over this area is about 0 mgal, which is a direct indication that the total mass in the crustal column of this area is almost equal to that in the standard crustal section. Accordingly, from the consideration given in Section 3.1., the density of the second layer should be related with H_t by,

$$\rho_2 = -\frac{(\rho_M-\rho_C)H_S-(H_t-H_2)(\rho_M-\rho_1)-H_2\rho_M-H_I(\rho_M-\rho_I)}{H_2}, \qquad (13)$$

where ρ_1, ρ_2 and ρ_M represent the density of the first layer, second layer and the mantle respectively. Other quantities are the same as previously defined. Although an intermediate layer is adopted here, its effect is very little, for $\rho_M-\rho_I$ is presumably very small. In this study, $H_I(\rho_M-\rho_I)$ is assumed to be 1 kmg/cm^3, but it need not necessarily be so. For the density in the first layer ρ_1, we take $\rho_1=2.74$ g/cm^3 which has been determined from $v_1=6$ km/sec and the Nafe-Drake curve. From Equations (11), (12) and (13), we can obtain various pairs of values for ρ_2 and v_2, which are tabulated by Table 3. From all these pairs, physi-

Table 3. True thickness of the crust and the density in the second layer for various values of the thickness H_2 and velocity v_2 of the second layer.

H_2 \ v_2	6 km/sec.	6.3	6.6	6.9	7.2	7.5
0 km	H_t=28.0 km $\rho_2=\infty$ g/cm^3	28.0 ∞	28.0 ∞	28.0 ∞	28.0 ∞	28.0 ∞
3	28.0 3.30	28.5 3.37	28.8 3.43	29.3 3.52	29.9 3.63	—
5	28.0 3.07	28.7 3.13	29.4 3.22	30.1 3.29	31.1 3.39	—
7	28.0 2.97	29.0 3.04	30.0 3.12	31.0 3.20	—	—
10	28.0 2.90	29.4 2.98	30.8 3.05	32.3 3.13	—	—
15	28.0 2.85	30.1 2.92	—	—	—	—

cally unacceptable ones should be excluded. By the $\rho-\alpha$ relations given in Section 2, it is clear that only the pairs which have $v_2=6.6\sim6.9$ km/sec, $H_2=7\sim10$ km, $\rho_2=3.00\sim3.15$ g/cm^3 and $H_t=30\sim32$ km are acceptable; no other pairs can be regarded as physically probable. The adoption of

different values for $H_I(\rho_M-\rho_I)$ and ρ_1 might change the results somewhat, but still it could be said that a 10 km thick second layer in which v_2 is 6.5~7 km/sec and ρ_2 is about 3.00 g/cm^3 could well explain the results obtained by both gravity and explosion studies. Whether the upper bound of this layer is acoustically well-defined or not is uncertain and it might be optional to call it the Conrad discontinuity.

4. Most probable crustal section in Japan

From the analysis in the previous section, we come to the conclusion that, (Fig. 9).

1) There is no appreciable difference in the value of the mean crustal density between the crustal section in this area and the standard section as given by Worzel and Shurbet.

2) The vertical distribution of the compressional wave velocity in the crust is very similar to that of the standard crust as given by Press.[14]

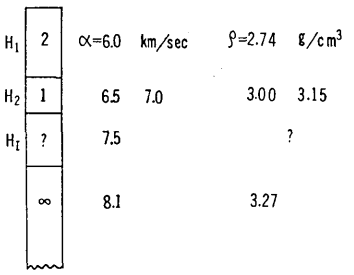

Fig. 9. Most probable crustal sections in Japan from the indications of gravity and explosion studies.

5. Most probable depth of Moho in Japan

From these conclusions, we can reasonably take the mean crustal density in Japan to be 2.84 g/cm^3, which is the same as that of the standard crustal section given by Worzel and Shurbet. Taking this value and extending it over the whole of Japan, we can determine the depth of the Mohorovičić discontinuity in Japan. As in the treatment in Section 2.2. we can obtain the mean depth of the Moho $D=H_1+H_2$ of the 1° squares, defined in Part 1 of this study, by the following formula,

$$D=H_S-\frac{H_I(\rho_M-\rho_I)}{\rho_M-\rho_O}-\frac{\Delta G}{2\pi k^2(\rho_M-\rho_O)}\ ,$$

where ΔG is the reduced Bouguer anomaly. If we substitute the values 2.84 g/cm^3 and 1 kmg/cm^3 for ρ_O and $H_I(\rho_M-\rho_I)$, D for all the 1° squares on land can be computed as shown by Table 4 and Fig. 10.

It should be noted here that these values may be somewhat affected by the two major assumptions we have made. First, the ratio of the

14) F. PRESS, *J. Geophys. Res.*, **65** (1960), 1039.

Table 4. Mean depth of Moho in kilometers for every 1° square on land derived from the reduced Bouguer anomalies ΔG given in Part 1 of this study.

1° square No.	Locality °E	°N	Depth of Moho $D=H_1+H_2$ km
6	142-143,	44-45	28.9
12	141-142,	43-44	27.6
13	142-143,	43-44	29.6
14	143-144,	43-44	30.2
15	144-145,	43-44	25.4
18	140-141,	42-43	28.3
19	141-142,	42-43	30.0
20	142-143,	42-43	31.1
21	143-144,	42-43	29.6
25	140-141,	41-42	26.3
26	141-142,	41-42	23,9
31	140-141,	40-41	28.3
32	141-142,	40-41	25.4
36	140-141,	39-40	28.6
37	141-142,	39-40	24.3
41	139-140,	38-39	28.5
42	140-141,	38-39	29.0
43	141-142,	38-39	24.8
48	138-139,	37-38	30.4
49	139-140,	37-38	30.8
50	140-141,	37-38	27.2
58	136-137,	36-37	30.6
59	137-138,	36-37	34.3
60	138-139,	36-37	32.8
61	139-140,	36-37	28.9
62	140-141,	36-37	22.8
66	132-133,	35-36	29.4
67	133-134,	35-36	30.3
68	134-135,	35-36	30.4
69	135-136,	35-36	30.6
70	136-137,	35-36	33.0
71	137-138,	35-36	32.0
72	138-139,	35-36	32.7
73	139-140,	35-36	31.3
74	140-141,	35-36	30.1
78	131-132,	34-35	31.0
79	132-133,	34-35	31.9
80	133-134,	34-35	30.5
81	134-135,	34-35	30.1
82	135-136,	34-35	30.2
83	136-137,	34-35	29.1
91	130-131,	33-34	29.9
92	131-132,	33-34	31.3
93	132-133,	33-34	31.9
94	133-134,	33-34	30.6
95	134-135,	33-34	29.9
96	135-136,	33-34	25.4
101	130-131,	32-33	27.6
102	131-132,	32-33	34.1
109	130-131,	31-32	29.9
110	131-132,	31-32	32.6

thickness of the first layer to that of the second layer has been assumed to be 2:1 for the whole of Japan. If this ratio does not hold everywhere, the mean density needed in the computation of D from ΔG should be changed, resulting in a different value of D. Secondly, since very little is known for the intermediate layer, there is no compelling reason for regarding it as a layer of uniform physical property and it can well be a transitional layer in which the physical parameters gradually vary from the crustal value just below the second layer to that of the normal mantle at the bottom. This seems very likely to be the case in some places. Concerning this point, more will be discussed in Part 3 of this study from the view-point of surface wave studies. In spite of these assumptions, the values given in Fig. 10 and Table 4 appear to be consistent with the general seismic results obtained by R.G.E.S. allowing for a possible increase of the seismic depth of about 10 per cent due to the layer masking.

In order to compile a contoured map showing the depth of the Mohorovičić discontinuity, the values D_{ij} determined at every grid point 1° apart are interpolated by the same method as given in Part 1 of this study.[15] Fig. 11 shows a contoured map of the depth of the Moho in Japan with a contour interval of 2 km.

In Fig. 10, Fig. 11 and Table 3, it can readily be seen that,

1) in Tohoku district, the crust becomes thinner from west to east as indicated by the R.G.E.S..

2) The crustal thickening is clearly seen in Chubu district reflecting the excessive mass of the central mountains. In this area the crustal thickness varies very abruptly from Chubu district to Kanto district (e.g. square No. (58) to square No. (62)). This might be one of the causes of the anomalous propagation of seismic waves in this area.

3) In San-in district, no abrupt change in the crustal thickness can be seen.

4) In Kyushu district there is a tendency of crustal thickening from west to east.

The variations of the depth of Moho given by the present analysis based on gravity data is appreciably smaller than that deduced by the surface wave studies by Aki,[16] and Kaminuma and Aki.[17] Probably, this is due to the fact that the surface wave results are very sensitive

15) H. KANAMORI, *loc. cit.*, 1).

16) K. AKI, *loc. cit.*, 10).

17) K. KAMINUMA and K. AKI, *loc. cit.*, 11).

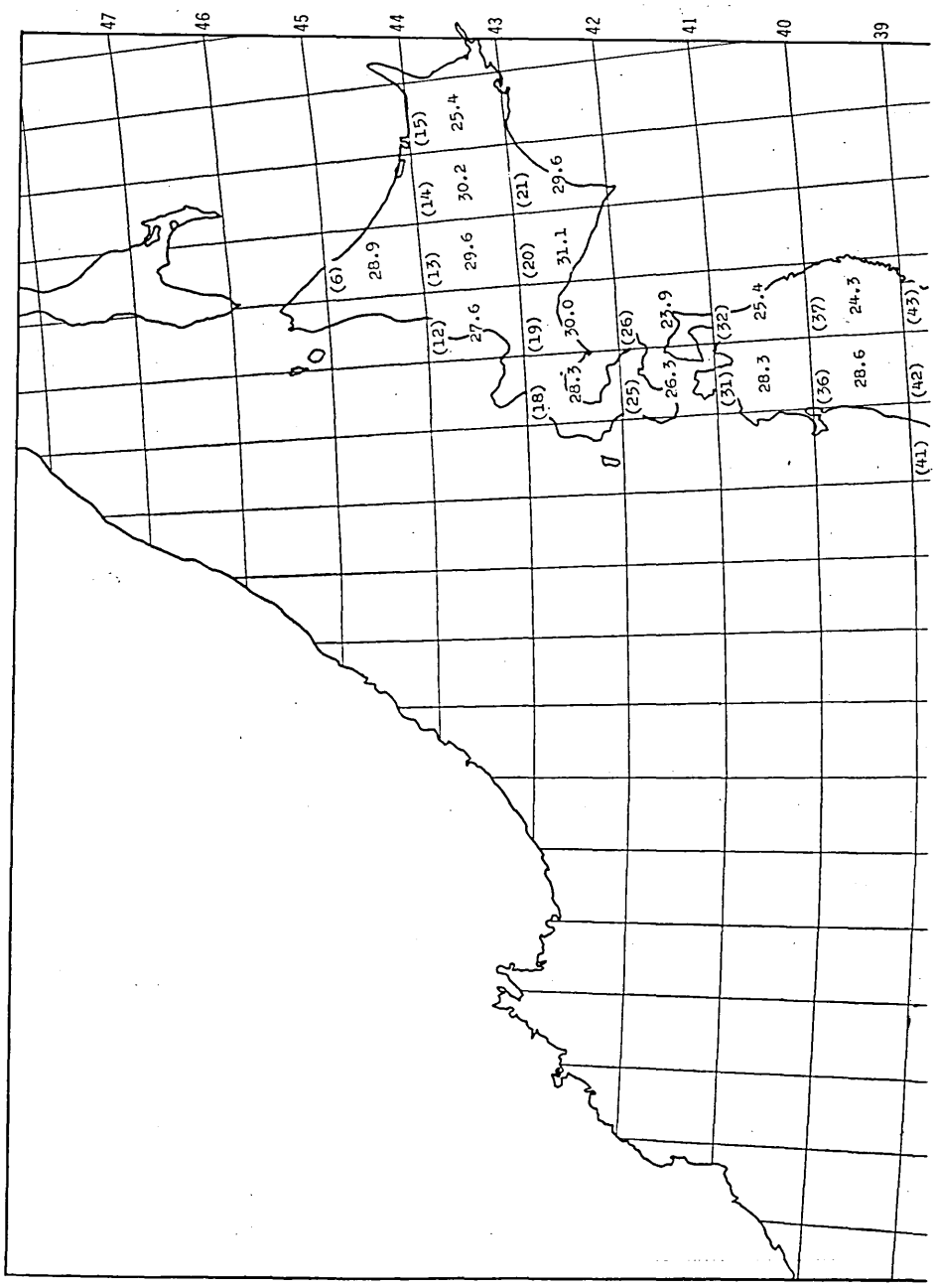

Fig. 10. Mean depth of Moho in kilometers for every 1° square on land

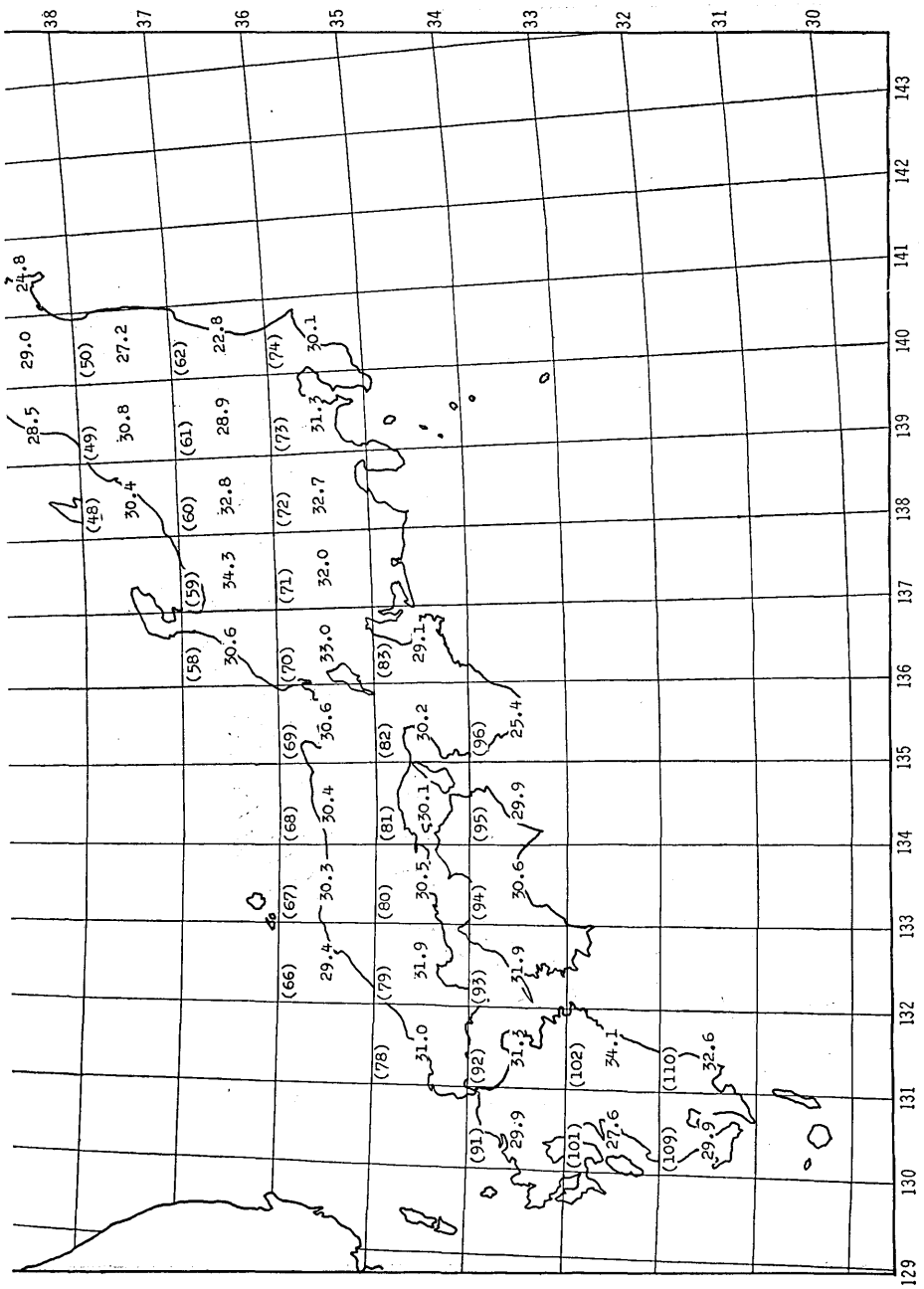

derived from the reduced Bouguer anomalies given in Part 1 of this study.

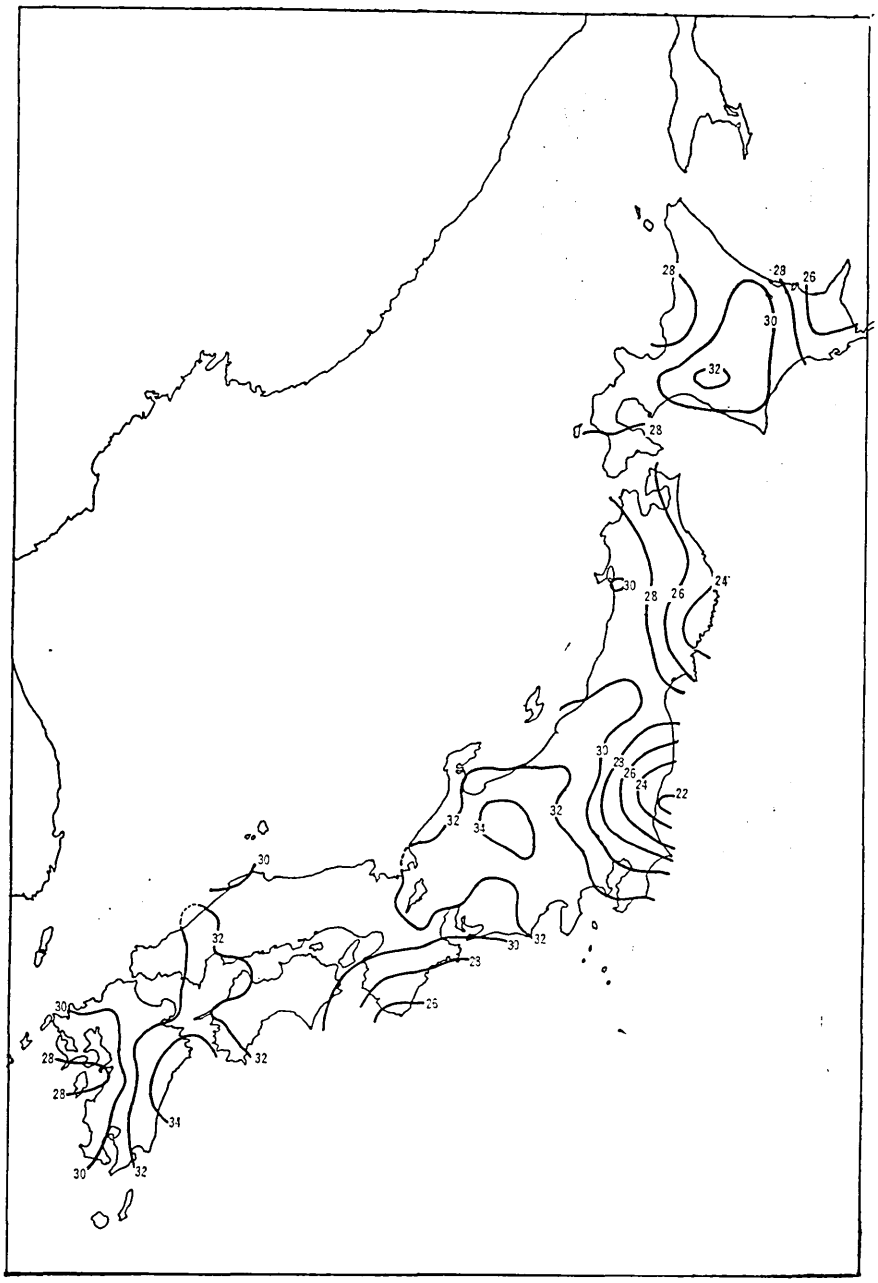

Fig. 11. Map of the depth in kilometers of the Mohorovičić discontinuity in Japan. The contour interval is 2 km. To convert to the crustal thickness, the mean topographic height over 1° lat. ×1° long. should be added to the value at each point.

to the shear velocity distribution in the crust and upper mantle. This point will also be discussed in Part 3.

It is a pleasure to acknowledge the advice and criticism of Prof. H. Takeuchi and Dr. S. Uyeda.

---

46. 日本の地殻とマントル上層部の構造

Part 2. 爆破地震動によつてきめられた構造と重力によつて決められた構造

東京大学理学部地球物理学教室 金森博雄

爆破地震動研究グループ (R.G.E.S.) によつて日本のクラストおよびマントル上層部の構造が推定されているが，これらはいくつかの仮定のもとに得られたいわゆる "seismic structure" である．またこの論文の Part 1 で決められた reduced Bouguer anomaly はいわゆる "gravity structure" を与えるものである．これらの二つの構造を結びつけるためには，P 波の速さ αと，密度 ρ の関係をいろいろの岩石，鉱物について知る必要がある．ここでは Birch らによつて得られた多くの岩石の sample についての測定結果をもとにして "seismic structure" と "gravity structure" を結びつけることを試みた．R.G.E.S. によつて導かれた構造は，クラストの中には速度勾配はないという仮定にもとずくものであるが，実際のクラストの中では，深部ほど P 波の速さが大きいと考えるのは弾性力学的には極めて考え易い．このようなクラストを考えると，クラストの厚さは，同一の初動の走時曲線に基ずいても R.G.E.S. によつて求められたものより約 10% ほど厚くなり得る．この論文では，中国地方の構造について，いわゆる masked layer を考えて，この地域での重力異常と，R.G.E.S. によつて得られた初動の走時曲線をもつとも合理的に説明し得るクラストのモデルを導いた．導かれたモデルはクラストの下部に $\alpha=6.6\sim7.0$ km/sec, $\rho=3.00$ g/cc 程度の層を考えるものであるが，この層の上の境界面がはつきりした不連続面であるか，あるいは遷移的に変化するものであるかは判らない．しかし，いずれにしても，このようなモデルは大陸において考えられているクラストのモデルとあまり違わないものである．

R.G.E.S. によつて得られた結果では，日本の Moho のすぐ下の P 波の速さは，7.5～7.9 km/sec で大陸における平均的な速さに較べてかなり遅い．このような P 波速度の遅い層が mantle のかなり深いところまで続いているものか，あるいは Moho 以下の比較的浅いところで，普通の速さをもつ層に変わつているのかについては，はつきりしたことはいえない．

Moho 以下の構造の変化が重力にあまり大きな影響をもたないことを仮定すると，Part-1 で求めた reduced Bouguer anomaly から日本における Moho の深さを求めることができる．このようにして得られた各地域の Moho の深さは，R.G.E.S. によつて得られたクラストの厚さよりどこでも約 10% 程度大きい．これは mask された層を考えることによつて説明できることであつて，その意味でかなり正しい深さを与えるものと考えられる．